Quasidivergency-free extraction of a slow positron beam from high magnetic fields

D. Gerola, W. B. Waeber, and M. Shi
Paul Scherrer Institute, CH-5232 Villigen PSI, Switzerland

S. J. Wang
Department of Physics, Wuhan University, Wuhan 430072, People's Republic of China

(Received 28 February 1995; accepted for publication 15 March 1995)

In a hybrid slow positron beam, extraction of the positrons from the magnetic field (~1 T for the PSI beam) to field-free space is a necessary operation. A theoretical and experimental demonstration is given which shows that the following proposed beam extraction method works as predicted: magnetic transport of the slow positrons down to field strengths of ~100 G and passage through an aperture grid of ~10 cm diameter in a field termination shield followed by some brightness enhancement stages. The simulation and measurement of the magnetic-field distributions along the beam axis show a steep drop down of the field from ~100 G to a few gauss within 1 cm of shield thickness and a quasiuniform spreading of the transverse field strength across the grid opening. Measurement of transmission and divergency (transverse energy) of the beam exiting the extraction aperture confirmed theoretical estimations and ray tracing calculations for the aperture design used to be of the order of 75% and 20 eV, respectively. These data as a function of field strength and beam energy are used for optimization of the final extraction aperture design (>85% transmission) to be used in the PSI high intensity beam facility.

I. INTRODUCTION

Whether a slow positron beam should be a magnetic beam or an electrostatic beam was mainly determined up to recently by the type of beam experiments that were intended to be performed.[1,2] For example, a standard diffraction experiment cannot be carried out in a magnetic field. Real "hybrid beams" which would place the radioisotope source in a transversally confining magnetic field and eventually would transport the positrons in electrostatically collimated beams to the sample situated in field-free space so far have not yet been realized. This question is certainly raised and maybe of importance in some of the high intensity positron beam projects which have been proposed[3–5] and which have been under development for the last few years,[6–8] because a high intensity facility might be planned to be used for an enlarged number of different types of beam experiments. A real hybrid beam of this kind needs extraction of the slow positron beam from the magnetic field, whatever its strength is at the position of the positron source, into field-free space, an operation which, as will be shown in this paper, can be realized in an efficient way. Moreover, electrostatic focusing of a magnetically guided positron beam is a very difficult operation and therefore not practical, i.e., any brightness enhancement operation, for example, can be performed efficiently in field-free space only.

The new method of positron beam production developed at PSI, which is partially based on an enhanced overall moderation efficiency, can be reduced essentially to three stages: (i) *premoderation*,[6] the stage of electromagnetic positron trapping and positron slowing-down, (ii) *field extraction*,[9] the stage of magnetic-field termination and "divergency-free" positron beam extraction into field-free space (subject of this paper), and (iii) *beam compression*,[10] the stage of electrostatic focusing and positron remoderation (brightness enhancement). This stage forms a usable monoenergetic beam with a very small transverse phase space of the order of 100 μm/50 mrad. The first two stages represent some new land. The corresponding experiments were crucial and decisive in the development of the project and they have been highly successful. These stages are actually guaranteed to reach in an initial step slow positron intensities of the order of 10^7 e^+/s (based on 1 Ci ^{58}Co) with a potential of stepwise upgrading[7,8] by several times 10^3 in the pilot facility presently under construction.

There have been two proposed methods for realizing the field extraction of the beam into field-free space. One is the phase-space shifter action after adiabatic magnetic transport of the beam to very low field (~3 G).[11] The other is the beam extraction by field termination through a magnetic shield with an aperture opening furnished by a magnetically conductive internal structure (magnetic grid).[9] In this paper we shall concentrate on the latter method. It will be shown that cylindrical symmetry is broken by the magnetic grid; thus it becomes possible to keep the *divergency* of the extracted beam small and at the same time to terminate the magnetic field nonadiabatically, allowing one to obtain a large *transmission* of the extraction aperture. Indeed, these are the main requirements for the subsequent beam focusing operation to be efficient, i.e., low transverse beam energy, nonadiabatic particle motion when passing through the aperture, and negligible magnetic-field strength on the exiting side of the aperture.

The following sections will discuss the basic concept and the extracted beam phase space, including simulations of the relevant parameters of the field distributions, the aperture design, and the particle trajectories. In further sections details

are given for the experimental determination of the transmission and the divergency of the used extraction aperture in the resulting fields of the chosen experimental configuration.

II. CONCEPT AND EXTRACTED BEAM PHASE SPACE

Within the frame of the relevant theorem governing the motion of charged particles in magnetic fields, this section describes the basic idea of field termination and nonadiabatic passage of the positron beam through such a field border region.

A. Theoretical considerations

Considering a set of positron trajectories passing through two subsequent surfaces S_1 and S_2 bounded, respectively, by the curves C_1 and C_2, the following relation holds:[12]

$$\oint_{C_1} \mathbf{P}\cdot d\mathbf{l} = \oint_{C_2} \mathbf{P}\cdot d\mathbf{l} \tag{1}$$

(where $\mathbf{P}=\mathbf{p}+e\mathbf{A}$ is the canonical momentum). From this relation, using the Stokes' theorem, it is possible to obtain a generalized form of Busch's theorem:

$$\oint_{C_1} \mathbf{p}\cdot d\mathbf{l} - \oint_{C_2} \mathbf{p}\cdot d\mathbf{l} = -e\int_{S_1} \mathbf{B}\cdot d\mathbf{S} + e\int_{S_2} \mathbf{B}\cdot d\mathbf{S}. \tag{2}$$

In the case of cylindrical symmetry (considering circular surfaces of radius r perpendicular to the z axis, the final magnetic field equal to zero, and neglecting the initial very small momentum of the particles) we obtain the Busch theorem[13] for which the final transverse momentum and energy, acquired by the particles traveling at a distance r from the axis and escaped from the magnetic field, are given by the following formulas:

$$p_\theta(r) = (e/2)(rB), \tag{3}$$

$$E_T^B(r) = (e^2/8m)r^2B^2 \tag{4}$$

(the suffix B indicates the contribution due to the magnetic field. The small initial transverse energy is neglected). Equation (3) introduces a correlation between p_θ and r such that the phase-space volume is the same as that of a source emitting in field-free space[14] (see Fig. 1). But unfortunately any kind of magnetic or electrostatic lens system can couple only p_r to r, so that the existing relation is practically useless for performing a focusing operation onto a remoderator foil[2] for brightness enhancement.

In electron optics it is very useful to introduce the r-θ diagram[15] (where $p_r = \theta\sqrt{2mE}$). The area Γ in this diagram is related to the brightness-per-volt of the beam[16] through the relation

$$\mathscr{B} = (4/\pi)^2 \frac{I}{\Gamma^2 E}, \tag{5}$$

where I is the beam intensity and $\Gamma^2 E$ is an invariant quantity, according to Liouville's theorem. For an isotropic source of radius r and emitting in field-free space, the area Γ is equal to $4r\sqrt{E_T/E}$, where E_T is the maximum transverse energy. Let us suppose that the magnetic field falls down to zero in a very short distance and a beam of radius r_b is

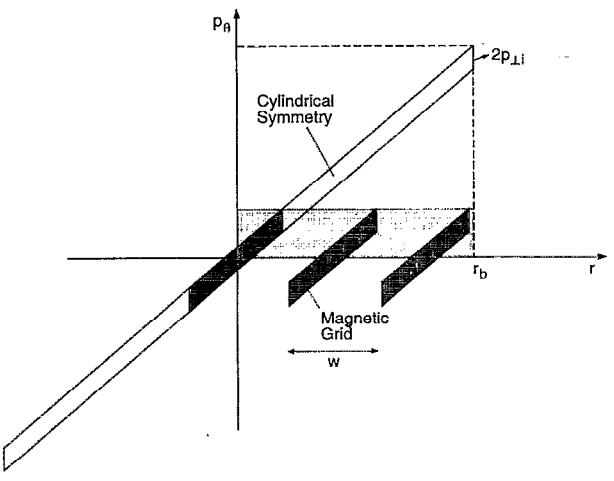

FIG. 1. The $p_\theta - r$ diagram of a beam extracted from the magnetic field in the cylindrical symmetric case and in the broken symmetry case of our special aperture. In the first case the slanted area is the same as of a beam emitted in field-free space. $p_{\perp i}$ represents the initial transverse momentum neglected in Eq. (3). In the second case p_θ is a periodic function of r (this is rigorously true only in the midplane between two bars, where the transverse momentum is added in the azimuthal direction). The two rectangles represent the area of an equivalent beam in the $r-\theta$ diagram.

extracted. In field-free space, the beam does not have the phase space of an isotropic source since the momentum is added in the azimuthal direction and it is related to the distance from the axis through Eq. (3). If we consider the outcoming beam like an isotropic source with a maximum transverse energy given by $E_T^B(r_b)$ and an area Γ equal to $4r_b\sqrt{E_T^B(r_b)/E}$, we overestimate its real phase-space volume. But this is necessary since, as mentioned before, it is not possible to take advantage of relation (3) using standard focusing devices. Hence from Eq. (5) we finally obtain a brightness-per-volt given by the expression

$$\mathscr{B} = \frac{I}{\pi^2 r_b^2 E_T^B(r_b)}. \tag{6}$$

From Eq. (4) and inserting the source radius r_0 in the field B_0, we obtain

$$\mathscr{B} = \frac{8m}{(\pi e)^2}\frac{I}{r_0^4 B_0^2} \tag{7}$$

[in the denominator of Eq. (7) and of the following Eq. (11) we have neglected the term representing the intrinsic phase space of the beam that limits the maximum value of the brightness-per-volt achievable]. This is the known expression for the brightness-per-volt of a source emitting in a magnetic field[12,17] and it is thus fixed by the initial source parameters. In the case of the beam under construction at PSI this value is very low because the magnetic field at the source position is extremely high[6] (tesla order). However, due to the correlation expressed by Eq. (3), the possibility of extraction of the beam with smaller transverse momentum is not physically forbidden.

The idea of the phase-space shifter method mentioned in the Introduction is to shift the slanted phase space in the $p_\theta - r$ diagram onto the r axis (introducing azimuthal com-

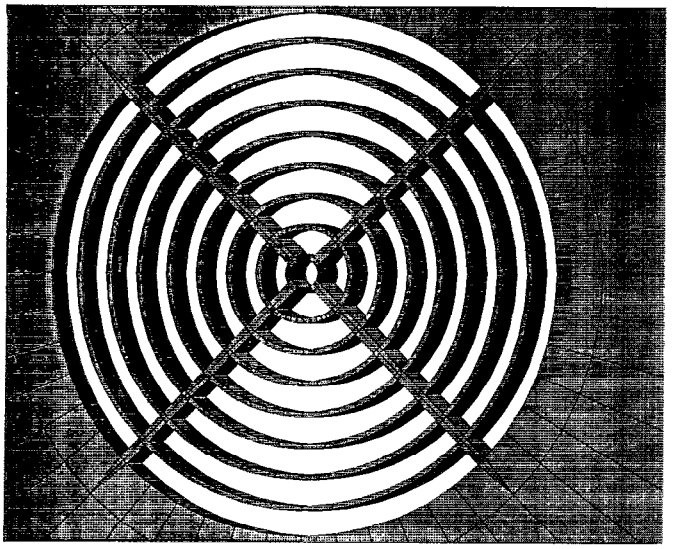

FIG. 2. The model used for the computer simulation of the aperture, at the center of a full iron disk of 60 cm diameter. The rings and the bars are 1 and 2 mm wide, respectively. The thickness of the shield is 1 cm. The total radius of the aperture is 5 cm. The dimensions of the manufactured shield were nearly the same except for some insignificant modifications.

ponents of the electric field with a special device), thus reducing the phase space of the equivalent beam in the $r-\theta$ picture.

The other device for field extraction, proposed by Shi *et al.*[9] and described in the following section, introduces a different correlation between transverse momentum and position (see Fig. 1), thus reducing the transverse energy added to the outcoming beam. In both methods it is impossible to conserve the number of particles. In the first this is due to irrotationality of the electric-field vector, while in the second, as shown below, the introduction of a magnetic grid for field termination results in an overall loss of cylindrical symmetry.

B. Field termination and aperture design

The idea is to use a kind of magnetic grid at the center of a full iron shield as illustrated in Fig. 2. The B field lines enter into the rings and the four radial bars guide them to the bulk structure of the shield. Now the Busch theorem *cannot* be applied to the overall circular area since the number of particles for sure will not be conserved: a fraction of positrons will hit the iron structure and never arrive to the final surface, S_2. But we can apply the general form of the Busch theorem *locally* using two parallel surfaces of equal shape, with respect to the open area between two rings, before and after the shield. Considering two rings far from the axis, separated by a distance w, with simple passages we obtain for the maximum transverse momentum and energy

$$p_\perp=(e/2)(wB), \tag{8}$$

$$E_T^B=(e^2/8m)w^2B^2. \tag{9}$$

Equation (8) can also be derived[9] by using the Lorentz equation and the conservation of the flux for determining the value of $B_r=wB/2d$ (d is the thickness of the shield), i.e.,

$$p_\perp=e\int v_z B_r\, dt\sim ewB/2. \tag{10}$$

Hence, the maximum transverse momentum can be reduced by a factor w/r_b with respect to the cylindrically symmetric case, and $p_\perp$ becomes a periodic function of r (with a pitch length equal to w) as shown in Fig. 1. The perpendicular momentum is not added in the azimuthal direction (except for positrons passing in the midplane between two bars). Nevertheless, if we consider, as in the previous section, the beam extracted like an isotropic source with the maximum transverse energy given by Eq. (9), we obtain a much smaller area in the $r-\theta$ diagram (see again Fig. 1). The beam brightness-per-volt is then given by

$$\mathscr{B}=\frac{8m}{(\pi e)^2}\frac{I}{r_0^2B_0w^2B}. \tag{11}$$

The brightness can be increased diminishing either the width w between two rings and/or the field B in front of the shield. Of course, the possibility of reducing B is limited by the difficulty in realizing a large device and more so by possible aberration effects of the electrostatic lens system for the subsequent focusing of a beam with a large diameter. Also, w has a lower limit imposed by practical considerations and the necessity of maximizing the transmission efficiency. In our case, for having acceptable dimensions of the shield to be placed inside the high-vacuum system and for reducing the complexity of the design, we have chosen the following parameters: $w=6$ mm and B ranging between 50 and 100 G. Since the initial source diameter is of the order of 1 cm in 1 T, the total diameter of the grid was fixed to 100 mm. With these data, from Eq. (9), we obtain a maximum transverse energy ranging from 19.8 to 79 eV.

In order that the particles can pass through the grid, they should not follow the field lines. This is easily achieved if the magnetic field changes rapidly in a distance much smaller[18] compared to the particle's pitch length (in a field of 100 G, the pitch lengths are 4.7 and 21.3 cm for particles of 500 eV and 10 keV, respectively). The first requirement of the shield, then, is that the magnetic field must drop down to zero in a distance of the order of 1 cm. The internal structure of the aperture then has the double function of reducing the transverse energy of the extracted beam and of terminating the field lines nonadiabatically. In order to optimize all the other aperture design parameters, a computer simulation analysis was done, and the results are discussed in the next section.

C. Simulation of the field distributions

The simulation work for designing the aperture was performed by using the OPERA-3D program based on the finite element method.[19] Two possibilities were available for the practical realization of the device: (i) to design a one piece shield that could be put inside the vacuum system or (ii) to couple a smaller iron aperture placed inside a vacuum tube, with an external larger shield. The second solution was not optimal since the gap between the two parts produced an appreciable leaking of the magnetic field. The remaining stray magnetic field of the order of 10 G (from an initial field strength of 100 G) would have made the subsequent focusing

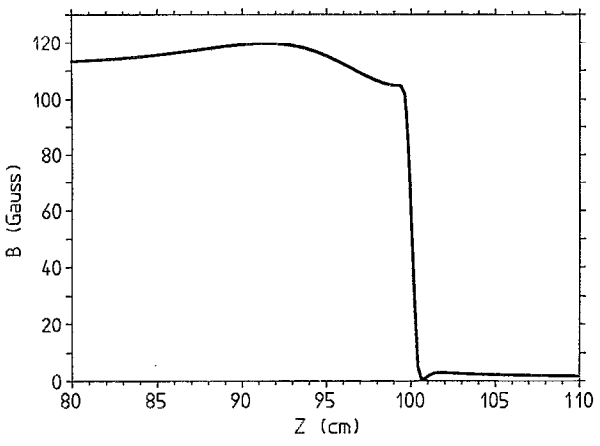

FIG. 3. The calculated B field distribution along the z axis. The shield is centered at $z=100.5$ cm. The magnetic field is produced by a long solenoid of 16 cm inner diameter, placed very close to the shield.

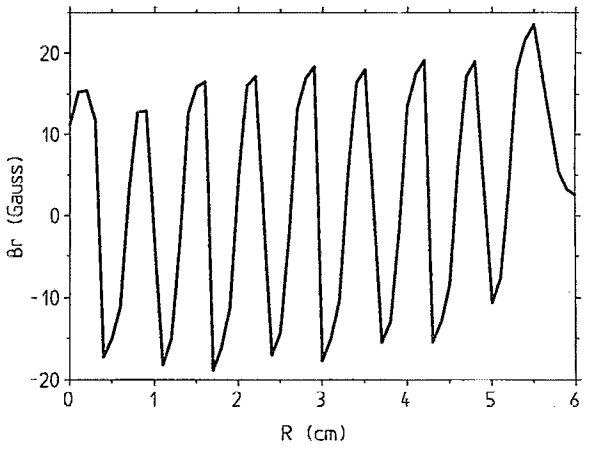

FIG. 4. Radial component of the magnetic field as a function of the radial distance from the axis at 1 mm distance from the shield, in the midplane between two bars. The result of the calculation in this case is not quantitatively correct due to the small number of mesh points at disposition between the rings.

operation difficult to perform.[10] Thus it was necessary to use a one piece shield. The main problem was then to optimize the ratio between the diameter of the solenoid producing the guiding magnetic field and the total diameter of the shield, in order to have the best reduction factor of field intensity with the minimum overall dimension. This ratio was found to be around 1/3. In the final design the shield diameter was 60 cm and the inner and the outer solenoid diameters were, respectively, 16 and 18 cm. An optimal thickness of the shield was found to be 1 cm. Dimensions of rings and bars were chosen in order to avoid saturation of the material and to maximize the ratio between open and total area of the structure (the bars and the rings were 2 and 1 mm in thickness, respectively). The relative magnetic permeability of the material used in the simulation was 4000 (characteristic of the so-called ARMCO iron that we used for the construction of the device).

The calculated B field distribution on the axis is shown in Fig. 3. It drops very rapidly from 110 down to 3.5 G (the precision of the calculation is of the order of ± 2 G). The radial component of the magnetic field along the radial direction, in the midsection between two bars, is shown in Fig. 4. It is periodically spread out over the whole aperture so that the maximum transverse momentum added to the particle is strongly reduced.

D. Ray tracing simulation

The limited number of finite elements in which the region between two rings was subdivided prevented the use of the same model for the ray tracing simulation. Thus a simplified geometry, a single rectangular slit (Fig. 5), was used so that the subdivision in the open space was fine enough for a more precise calculation. The results of this simulation are presented in Table I.

Some considerations are necessary, also in view of the discussion of the experimental results obtained. We observe that, from the previous theoretical consideration, the maximum transverse energy does not directly depend on the incident energy of the particle, as long as the transmission efficiency remains constant. But the transmission efficiency is a function of the incident energy. In fact, in this geometry, if the motion is nonadiabatic, the transverse momentum is added mainly in a direction parallel to the long side of the slit, so that the particles do not bump into the iron (see Fig. 5). But for low energies some of the positrons will tend to follow the field lines or they will acquire a component of the momentum parallel to the short side of the slit and thus they will hit the shield. This can be seen in Table I where the transverse energy is decomposed into two parts, E_{Tx} and E_{Ty}, related to the motion in the x and y direction, respectively. At high energy, E_{Ty} is negligible and the transmission efficiency has the maximum value. At low energy only the particles within an effective width less than w will be transmitted with a reduced transverse energy; the transverse energy at high incident energy is very close to the theoretical estimation (see Sec. II B). Both the transmission efficiency and the transverse energy monotonically decrease at lower incident energies (for the magnetic field of the order of 100 G).

III. MEASUREMENT OF THE TRANSMISSION AND DIVERGENCY

The basic measurements of the transmission and the divergency of the extraction aperture are fairly simple. However, the realization of the required field and charged particle beam conditions, as discussed in the previous sections, demands nontrivial efforts for the experimental setup which will be shown in this section.

A. Experimental setup

The experimental setup for measuring the performance of the shield and the extraction aperture is shown in Fig. 6. The aperture, as already mentioned, was produced from a 60 cm diameter disk of ARMCO iron, of 1 cm thickness, by a spark erosion process. Vacuum annealing for 4 h was done for restoring the magnetic properties of the material. In the final design, with nonsignificant differences with respect to the model used for the simulation, the overall diameter of the

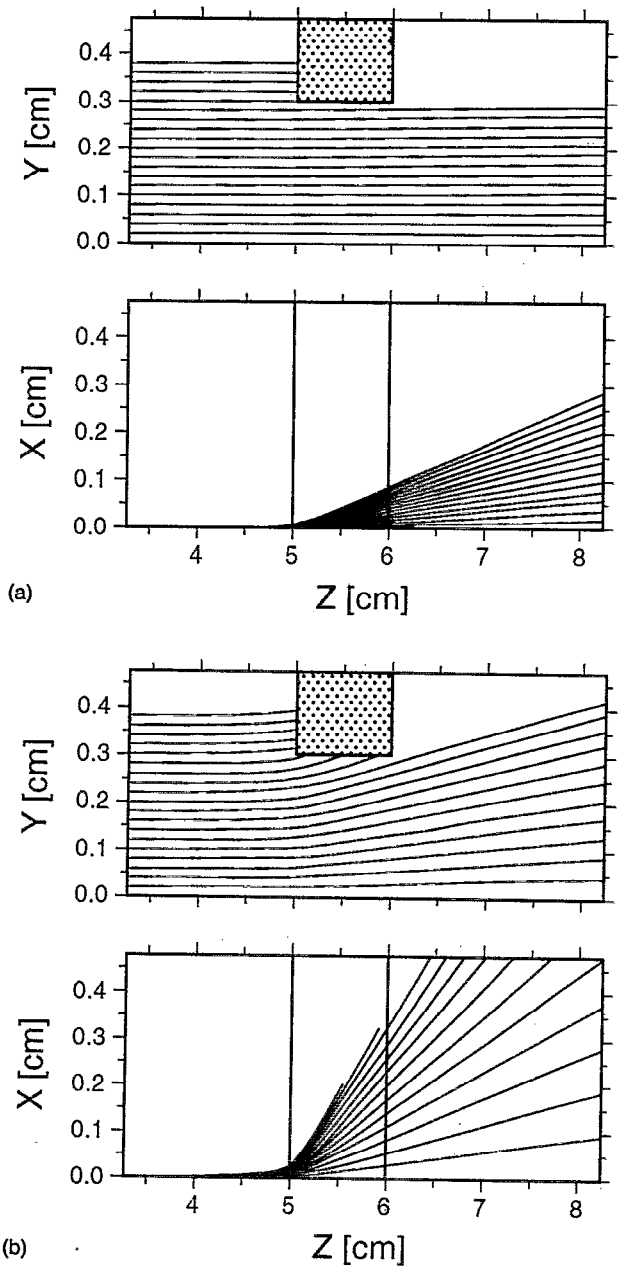

FIG. 5. (a) Trajectories for an ensemble of particles with an incident energy of 10 keV, passing through a rectangular slit as seen from the yz and xz plane (z is the beam axis). The long side of the slit (3 cm long) is parallel to the x axis while the short side (6 mm long) is parallel to the y axis. The shield is centered at $z=5.5$ cm and it is 1 cm thick. The initial magnetic field is 106 G. The incoming trajectories lie in the yz plane, whereas the exiting trajectories in the high-energy case lie in planes parallel to the xz plane. (b) As before but with an incident energy of 500 eV. In this case more particles, following the field lines, bump into the iron.

grid was 118 mm. Measurement of the shielding effect gave a reduction from 95 down to 6 G and from 80 down to 4 G, which within the error is not so far from the computer calculation result. The smaller reduction is probably due to the difference in the relative permeability of the real material compared to the value used in the calculation.

The device was tested by using an electron gun, placed between solenoids, producing a field of the order of 1 kG. The beam was mounted on a xy stage so that we could scan the beam across the aperture. It is necessary that the beam exiting from the gun reaches the aperture with an initially zero transverse momentum so that we can measure only the transverse energy introduced in the field extraction operation. Since the electrons, isotropically emitted from the gun, spiral in the magnetic field, for realizing this collimation we placed an electrostatic mirror just after the gun. Applying the mirror voltage V_m such that $eV_m=E-\epsilon$ (E is the total energy of the electrons), only particles with a maximum transverse energy less than ϵ can pass it. Moreover, in going from the high magnetic field, where the accelerator is placed, to the lower magnetic field, this transverse energy is reduced by a factor equal to the ratio between the field intensities (about 10 for this configuration). In our case, we estimated an initial transverse energy of only a few electron volts, much smaller than the one added by the aperture of the order of a few tens of electron volts (see Secs. II B and II D). By using this mirror we were able to reduce the beam spot size in front of the aperture to very small dimensions (order of 1 mm) owing to the radial electric potential distribution of the accelerator rings not being uniform.

B. Experimental results

We obtained the transverse energy by measuring the divergency angle of the exiting beam on a microchannel plate placed at a distance L from the shield. If the collimated beam passes very close to a ring, it acquires the maximum momentum and it travels toward the detector along a line forming a certain angle with respect to the incoming beam direction. Its final position can be observed on a phosphor screen. In moving toward the center of the gap between two rings, the divergency angle should decrease to zero and then increase again to its maximum value, but with an opposite sign due to the change in the field direction (see Fig. 4). In Fig. 7 the movement of the spot on the screen during a radial scan across several rings is shown. If the incident beam passes across an iron ring, the spot jumps to a different position. From elementary geometrical considerations, the divergency angle is related to the distance between these two positions, Δ, simply by $\theta=\arctan(\Delta/2L)$. The maximum transverse energy is then given by $E_T=E\sin^2\theta$.

The transmission efficiency was determined by measuring the beam current in Faraday cups, which could be moved into the beam line with a linear manipulator, before and after the aperture, and taking the ratio between these two measurements. This procedure was repeated for different positions along the radial direction. By scanning over several complete ring openings these ratios have been averaged for obtaining the transmission efficiency.

Divergency and transmission efficiencies were determined as a function of the incident beam energy and for three different values of the magnetic field. We concentrated our attention on the aperture region between two bars and in particular from the second to the fifth ring. Within experimental error, the measured values of the maximum transverse energy were nearly the same for the different rings. The averaged results are shown in Fig. 8 and Table II. The maximum transverse energy at high incident energy is very close to the simulated and estimated values. Moreover, the expected monotonic decrease with the incident energy is re-

TABLE I. Result of the simulation of the rectangular slit. The values of E_T are reported for different incident energies E and two magnetic fields. E_{Tx} and E_{Ty} are the contributions to the transverse energy due to the motion in the x and y directions. When the motion is completely nonadiabatic E_{Ty} is nearly zero. The efficiency of the slit is the ratio between the effective area and the total open area (since at 0.2 mm from the iron the field distribution is not reliable, the value of 93% reported could be considered a lower limit). In the last column we have an extrapolated value of the efficiency of our aperture considering that the ratio between the open area and the total area is 0.86.

B (G)	E (keV)	E_T (eV)	E_{Tx} (eV)	E_{Ty} (eV)	efficiency slit (%)	efficiency grid (%)
	0.5	53.6	52.4	1.2	77	66
	1.0	68.4	67.6	0.8	87	74
106	3.0	77.2	76.9	0.3	>93	>80
	6.0	77.3	77.1	0.2	>93	>80
	10.0	77.5	77.4	0.1	>93	>80
	0.5	18.7	18.6	0.1		
	1.0	19.3	19.25	0.05		
53	3.0	19.5	19.5	0.0	>93	>80
	6.0	19.6	19.6	0.0		
	10.0	19.7	19.7	0.0		

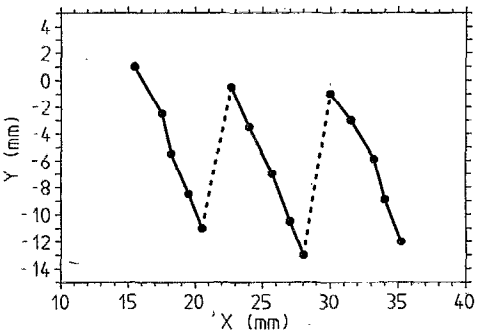

FIG. 7. Movement of the beam spot on the phosphorous screen during a scan in the radial direction in the region between two bars. (x, y, and z are Cartesian coordinates with the incident beam axis being parallel the z axis). The exiting beam is mainly deflected in the azimuthal direction and the divergency is maximum when the positrons are very close to the ring. In the middle between two rings the beam should be nearly unperturbated and in moving toward the other ring it is deflected in the opposite direction. When the beam passes over a ring it jumps to a completely different position (dotted lines) at a distance Δ from the previous one. Δ is related to the transverse energy.

produced (see Sec. II D). The transmission efficiency also shows the same trend but the values obtained, even if significantly higher, are somewhat smaller when compared to those deduced from the ray tracing calculations.

The discrepancy could be attributed, first, to some systematic errors in the measurement and, second, to the difference between the single slit geometry (see Sec. II D) and the more complex design of our system (see Fig. 2). As for the first point, for having a more stable current in the Faraday cup we were forced to release the collimation condition so that a noncollimated initial beam was used for the transmission measurements (in contrast, very good collimation was possible for the measurement of the divergency, since fluctuations in the beam current did not prevent the reading of the spot position on the phosphor screen). So already incident spiraling electrons were used, increasing the probability of hitting the shield. About the second point, in our geometry particles with azimuthal momentum could hit the inner surface of the rings due to their curvature. Hence, the values obtained represent a lower limit of the transmission efficiency and the possibility of performing a more precise measurement would probably increase these values closer to the theoretical level.

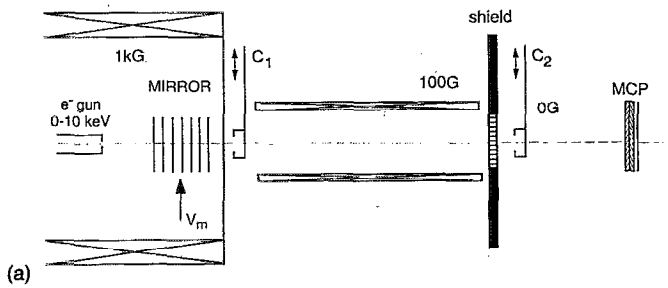

(a)

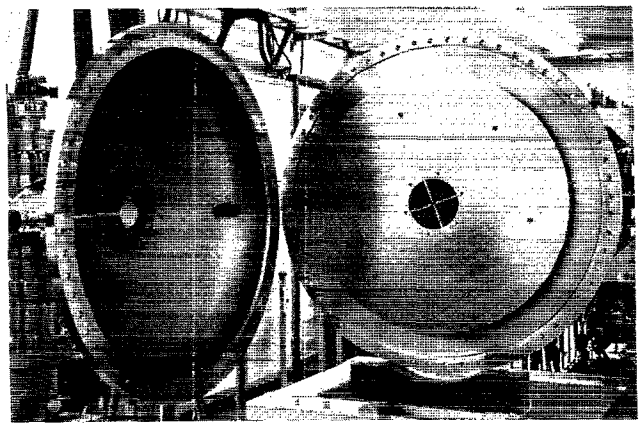

(b)

FIG. 6. (a) The experimental setup, C_1 and C_2 are Faraday cups that can be moved in and out of the beam, used for the determination of the transmission efficiency, by measuring the integrated currents on the cups. The microchannel plate (MCP) with phosphorous screen was used to measure the divergency. (b) Close-up of the inside of a large flange chamber. The right part shows the shield with the extraction aperture. The left part shows the MCP and the Faraday cup C_2 in front of it.

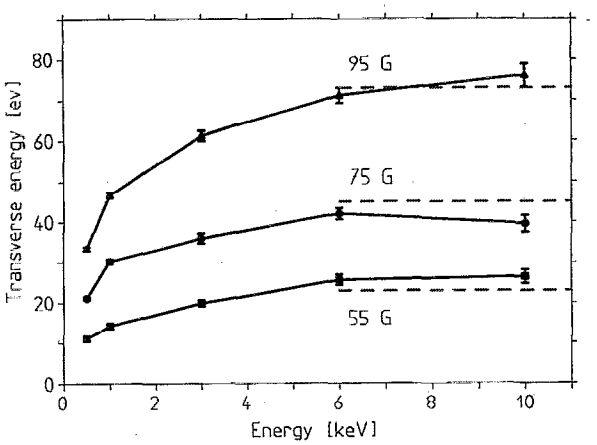

FIG. 8. Transverse energy vs initial beam energy and magnetic field. The horizontal lines indicate the calculated maximum transverse energy for the corresponding fields.

TABLE II. Measured transmission efficiency as a function of the incident energy and for two different values of the magnetic field. The big errors are due to the beam current instability.

	Efficiency (%)	
Energy (keV)	55(G)	75(G)
1	52±3	53± 4
3	69±6	66± 5
10		77±12

IV. POSSIBLE IMPROVEMENTS

We have experimentally shown that the aperture used gives satisfactory and predictable results. A transmission larger than 75% is achievable, and according to the magnetic-field intensity we obtain a transverse energy from 20 to 80 eV for 50 and 100 G, respectively.

The acceptable limit for the transverse energy depends, of course, on the subsequent possibility of electrostatically focusing the extracted beam onto a small remoderator foil. For a pure electrostatic beam with a source diameter of 1 cm, the factor $\Gamma\sqrt{E}$ is about 1 cm $eV^{1/2}$. In our specific case, where the source is placed in a 1 T field, extraction of the beam without any precaution would result in a $\Gamma\sqrt{E}$ of 1.5×10^3 cm $eV^{1/2}$. Such a phase space makes any kind of focusing operation impossible. Our tested special device would give a value of 130 cm $eV^{1/2}$, with a brightness-per-volt increased by more than two orders of magnitude. Despite this strong reduction of Γ, standard electrostatic lens systems cannot be used in the remoderation stage. For that reason, in parallel to the shield development, a new and unusual electrostatic lens system, placed just after the shield, was studied.[10] The main result is that our beam can be focused down to a spot where 70% of the positrons are inside a diameter of 8 mm and with a final incident energy of 7.5 keV. Of course this performance would be even better for an extracted beam with smaller phase-space area. It is then still important to improve the aperture design, not only for increasing its transmission efficiency, but also to improve the area in the r-θ diagram.

Based on the simulation results of the rectangular slit, we shall use an aperture of 120 mm diameter filled with simple parallel bars. Since the momentum is added mainly in a direction parallel to the bars, bumping of positrons into the iron should be minimized (see Sec. II D). Decreasing w to 4 mm, we can have a transverse energy of 20 eV for a magnetic field of 75 G. A thickness of the iron bars of 0.5 mm should be enough for avoiding saturation of the material. In this way a transmission efficiency of ~85% can be achieved and the final spot size on the remoderator should be 9 mm for the whole beam and 4.5 mm for 70% of it.

This work makes it possible to break with the tradition of setting up pure magnetic or pure electrostatic positron beams. Real *hybrid beams* can be realized because efficient interfaces between magnetic and electrostatic beam sections guarantee that intensity losses can be minimized, and the beam phase space can be transformed into acceptable dimensions required for subsequent beam compression operations. Application of this beam extraction method is not limited to source/moderator in high magnetic-field situations. In fact, any conventional, magnetically collimated source-moderator positron beam production scheme could be turned into an electrostatic beam by employing the quasidivergency-free beam extraction technique. Further reaching applications are indicated in any B-E charged particle beam transport configurations, for example, in accelerator technology.

ACKNOWLEDGMENTS

This work is partially supported by the Swiss Science Research Nationalfonds. We wish to acknowledge D. Taqqu and K. F. Canter for their constant interest and for fruitful discussions.

[1] P. Schultz and K. G. Lynn, Rev. Mod. Phys. **60**, 701 (1988).
[2] K. F. Canter and A. P. Mills, Can. J. Phys. **60**, 551 (1982).
[3] D. Taqqu, Helv. Phys. Acta **63**, 442 (1990).
[4] B. L. Brown, A. Denison, H. Makowitz, D. Gidley, B. Frieze, H. Griffin, and P. Encarnación, Am. Inst. Phys. Conf. Proc. **303**, 289 (1994).
[5] L. D. Hulett and C. C. Eberle, Contribution to the 10th International Conference on Positron Annihilation, Bejing 1994.
[6] M. Shi, W. Waeber, G. Gerola, U. Zimmerman, and D. Taqqu, Nucl. Instrum. Methods A **349**, 8 (1994).
[7] D. Gerola, W. B. Waeber, and M. Shi, Nucl. Instrum. Methods (in press).
[8] W. B. Waeber, M. Shi, and D. Gerola, Materials Science Forum, Vols. 175–178, 115 (1995).
[9] M. Shi, D. Gerola, W. B. Waber, and U. Zimmermann, Appl. Surf. Sci. **85**, 143 (1995).
[10] D. Gerola, W. B. Waeber, and M. Shi, Appl. Surf. Sci. **85**, 106 (1995).
[11] D. Taqqu, PSI Report No. 68, edited by W. B Waeber, D. Taqqu, U. Zimmermann, and G. Solt, 1990, p. 75.
[12] D. T. Pierce, C. E. Kuyatt, and R. J. Celotta, Rev. Sci. Instrum. **50**, 1467 (1979).
[13] J. D. Lawson, *The Physics of Charged Particle Beams* (Clarendon, Oxford, 1977), p. 16.
[14] D. Taqqu, Hyperfine Interact. **76**, 285 (1993).
[15] A. P. Banford, *The Transport of Charged Particle Beams* (Spon, London, 1966), pp. 9–19.
[16] J. H. Fink and B. W. Schumacher, Nucl. Instrum. Methods **130**, 353 (1975).
[17] V. W. Hughes, R. L. Long, M. S. Lubell, M. Posner, and W. Raith, Phys. Rev. A **5**, 195 (1972).
[18] B. Lehnert, *Dynamics of Charged Particles* (North-Holland, Amsterdam, 1964), p. 43.
[19] OPERA-3D, Vector Field Limited, Oxford.